



**POLITECNICO  
DI MILANO**

Department of Mechanical Engineering

TOPOLOGY OPTIMIZATION

---

**Topology Optimization of the Hub  
Carrier of an Ultra-efficient  
Lightweight Battery Electric Vehicle**

*STUDENT*

Gabriele Avi, 276 004

*TEACHER*

Prof. Ballo Federico Maria

Academic Year 2024 - 2025

## LIST OF FIGURES

2.1	Vehicle Asteria . . . . .	1
2.2	Double-wishbone suspension . . . . .	2
3.1	Design and non-design domain of the hub carrier . . . . .	2
4.1	Schematics used to approximate the boundary conditions . . . . .	3
4.2	Schematic of Constraint . . . . .	3
5.1	The six loading conditions . . . . .	4
7.1	Toe and camber angles . . . . .	5
9.1	Percentage distribution of the continuous normalised density of the elements . .	6
9.2	FEM with the magnitude of rotation for m.f. 0.4 . . . . .	7
9.3	Optimized structure for m.f. 0.4 . . . . .	7
9.4	FEM with the magnitude of rotation for m.f. 0.2 . . . . .	7
9.5	Optimized structure for m.f. 0.2 . . . . .	8
9.6	Results for the 2 studied cases . . . . .	8
9.7	Masses and masses fraction of the designs . . . . .	8
9.8	Refine structure for m.f. 0.4 . . . . .	9
9.9	Refine structure for m.f. 0.2 . . . . .	9
10.1	FEAs of the loading conditions for m.f. 0.4 . . . . .	10
10.2	FEAs of the loading conditions for m.f. 0.2 . . . . .	11
10.3	Stresses variation for the loading conditions . . . . .	12

## CONTENTS

<b>1 Abstract</b>	<b>1</b>
<b>2 Introduction</b>	<b>1</b>
<b>3 Design domain</b>	<b>2</b>
<b>4 Boundary conditions</b>	<b>3</b>
<b>5 Loading conditions</b>	<b>3</b>
<b>6 Material</b>	<b>5</b>
<b>7 Optimization problem</b>	<b>5</b>
<b>8 Methods</b>	<b>6</b>
<b>9 Results and discussions</b>	<b>6</b>
9.0.1 Case 1 (mass fraction 0.4) . . . . .	7
9.0.2 Case 2 (mass fraction 0.2) . . . . .	7
<b>10 FEA - stresses analysis</b>	<b>10</b>
<b>11 Conclusions</b>	<b>12</b>

## 1 ABSTRACT

This report looks at a topology optimization of a real component used in an high-efficiency vehicle of the Shell Eco-marathon team at Politecnico di Milano. The aim of the analysis is to maximize the hub carrier stiffness and minimize the weight, considering different loading conditions at which the car could be subjected during its life. All exploiting the commercial software Altair Hyperworks for the optimization and the FEAs and Altair Inspire for the surface wrapping in post-processing.

## 2 INTRODUCTION

The vehicle designed and manufactured by the team at Politecnico di Milano is called “Asteria” and belongs to the urban concept class, which includes vehicles with architecture inspired by small city cars. The electric drive train is powered by a 48 V lithium-ion battery pack for an overall nominal power of 400 W.



Figure 2.1. Vehicle Asteria

Since the aim of the competition is to complete the race using the least amount of energy, minimizing the energy dissipation became a crucial aspect. For this reason, a sensitivity analysis was done, revealing that mass is the most influential parameter on energy consumption. Hence, the aim of the project is to optimize the structural layout of the hub carrier in order to maximize the structural stiffness with the least amount of mass.

As said before, the component under analysis is the hub carrier which has three main functions:

- it closes the kinematic loop made by the two control arms;
- it receives the inputs from the steering rod and transfers them to the wheel;
- it bears the static and dynamic loads coming from the road and the brake caliper.

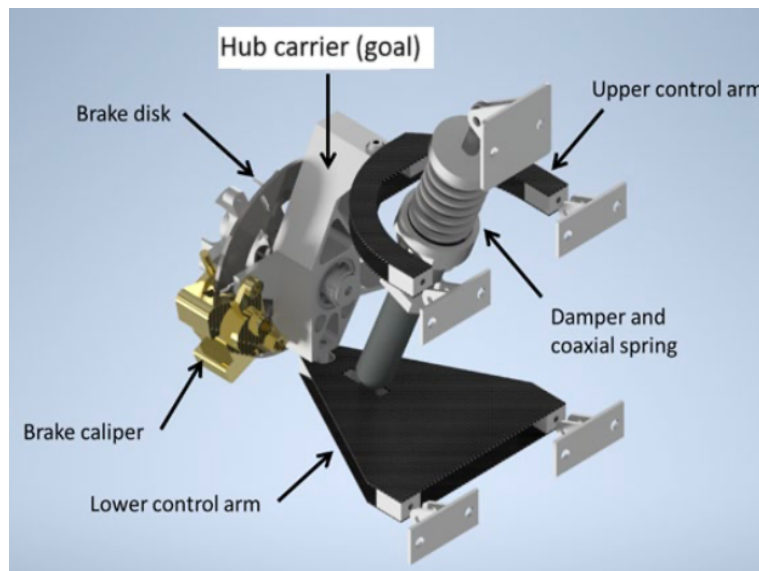


Figure 2.2. Double-wishbone suspension

The optimization process was divided into three main steps: the pre-processing, in which design domain, boundary conditions and constraints were defined, the effective optimization and the final post-processing with the discussion of the results with respect to the requirements.

### 3 DESIGN DOMAIN

In order to optimize the structure and preserve the features of the component, it is necessary to define the so called “non-design domain”. It represents functional surfaces (attachments) that must be preserved during the iterations. In the figure below it is shown the geometry of the hub carrier, where the red volumes represent portions of non design domain, whilst the blue one in the design domain (that can be optimized).

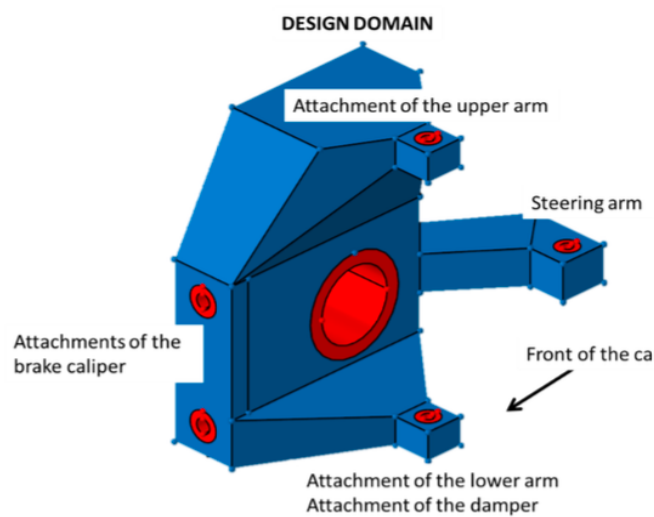


Figure 3.1. Design and non-design domain of the hub carrier

## 4 BOUNDARY CONDITIONS

The initial boundary conditions of the system can be schematized at a first approximation as follows:

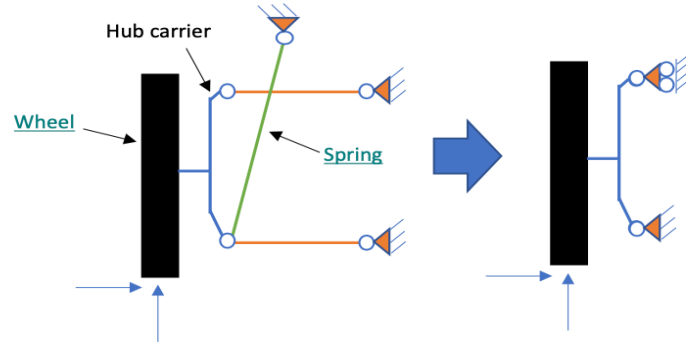


Figure 4.1. Schematics used to approximate the boundary conditions

In the specific, the upper attachment is free to move along Z direction (X and Y are constrained), the lower attachment, due to the damper and spring reactions is not free to move (X, Y and Z are constrained), and lastly the steering arm is linked to the steering rod, which constraints the displacement of the connection point only in the Y direction (X and Z are free).

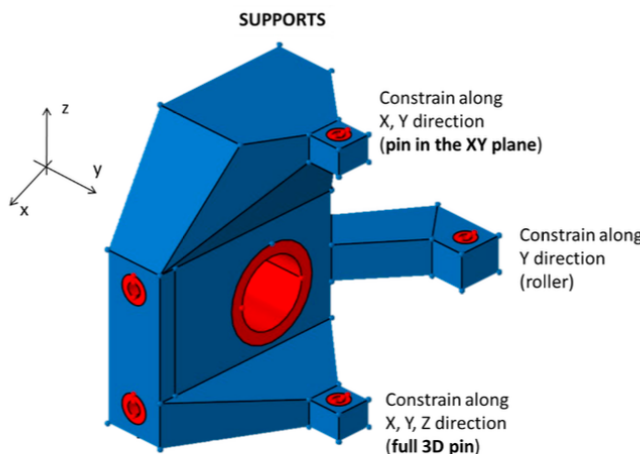


Figure 7 - Constraints.

Figure 4.2. Schematic of Constraint

Finally, the system end up with 6 degrees of constraint.

## 5 LOADING CONDITIONS

In order to realize the best and realistic optimization, as said before, it was necessary to define the loads at which the vehicle will be subjected during its life. Six different loading cases was used:

1. *Pure rolling*, it means that the hub carrier has to sustain only the weight of the car which is equal to 160 kg. It results in a total vertical force of 1600 N, which can be equally distributed on four wheels, with 400 N per each;
2. *Braking*, during braking, a load transfer occurs from the rear to the front axle, in this way the load due to the mass increases (1300 N). The tangential force caused by disc friction is transferred to the brake calliper's fixtures resulting in 700 N, and a final longitudinal braking force equal to 200 N is applied at the center of the hub carrier;
3. *Internal turn*, the car is steering and the hub carrier is internal to the curve. During this situation the load transfers from the inside wheel to the outside wheel, so in this case the right hub carrier is less stressed than the left one. Lateral acceleration generates tangential forces at the point of contact (on the tire), which are transported to the hub carrier and result in moments;
4. *External turn*, this is the case of internal turn but with the opposite sign of the forces/moment, with the difference that now it is the most stressed situation with higher load due to the mass;
5. *Internal obstacle*, these load cases simulate the hing of the wheel with an obstacle. The obstacle is generally a curb or a hole;
6. *External obstacle*, the opposite case, when the obstacle is hit by the external side of the front right wheel as for example a curb.

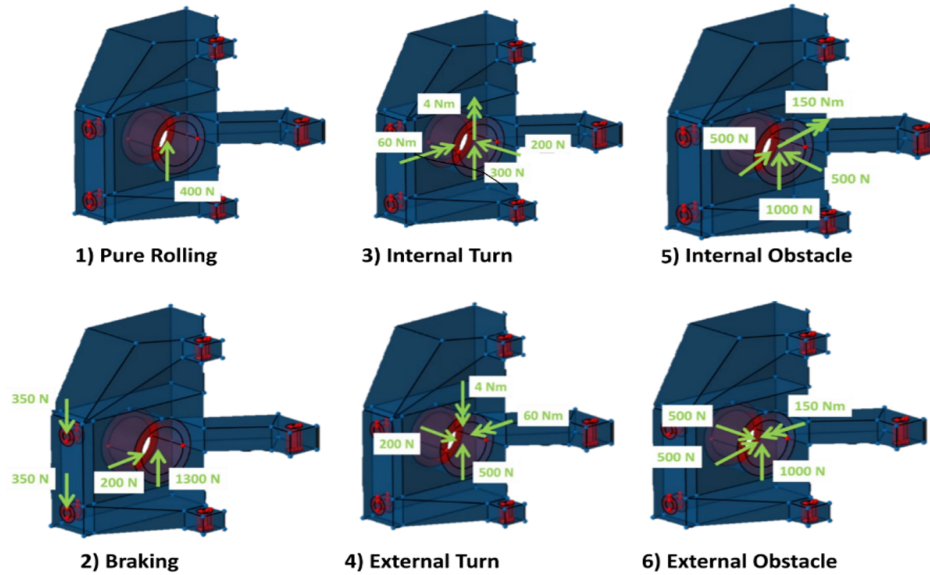


Figure 5.1. The six loading conditions

## 6 MATERIAL

The reference material used for this component is Aluminium 6061 T6, with densities  $\rho = 2700 \text{ kg/m}^3$ , Young module  $E = 70 \text{ GPa}$  and proof strength  $Y_s = 270 \text{ MPa}$ . It is modeled as an isotropic linear elastic material during the optimization process and FEA. Aluminium because it is the best trade off between stiffness and density.

## 7 OPTIMIZATION PROBLEM

The problem was the minimization of the weighted compliance of the six loads, with constraints on the maximum mass fraction and on the camber and toe stiffness. The mass fraction constraint was reasonably chosen, whilst the stiffness constraints were provided. It was also important to implement manufacturing constraints in order to obtain a structure which can be actually produced. For this case a draw (forging) along Y direction was imposed. The solid normalized density  $\rho$  was chosen as design variable. The problem and its constraints are summarized below:

$$\begin{cases} \min(\rho) \text{ weighted compliance} \\ \text{s.t.} \begin{cases} \text{mass fraction} \leq [0.2, 0.4] \text{ initial mass} \\ \text{toe stiffness} > 84000 \text{ Nm/rad} \\ \text{camber stiffness} > 160000 \text{ Nm/rad} \\ \text{forging constraint} \end{cases} \end{cases}$$

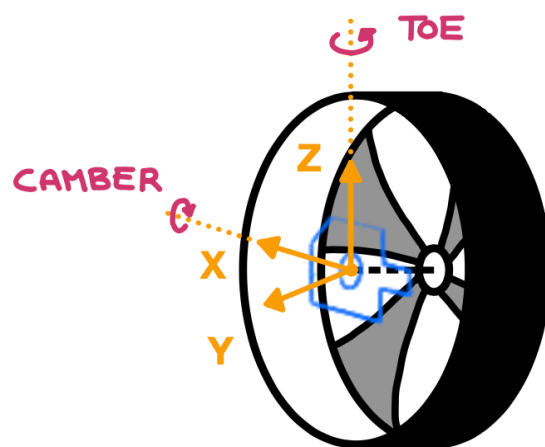


Figure 7.1. Toe and camber angles

## 8 METHODS

The project started with the pre-processing, i.e. the geometry of the piece was imported into Altair HyperMesh, where it was possible to assign the material properties and the 2 separate domains (the design and non-design). Both of them were meshed with a 2 mm size, rigid elements and boundary conditions were defined in order to apply the loads.

The next step was the optimization process, which was done considering 2 levels of mass fraction: 0.4 and 0.2. This was due to the fact that a comparison between these 2 cases was necessary to better understand how the mass fraction affects the results and how to choose the best option. Furthermore, a *draw* (forging) along Y direction was chosen as a manufacturing constraint to obtain a structure which can be actually achievable. Choosing forging over extrusion for an optimized part can be advantageous due to higher material strength, as forging refines the grain structure and enhances mechanical properties. It also offers better fatigue resistance, making it ideal for load-bearing components. Additionally, forging allows for greater design flexibility in complex geometries and can eliminate the need for extensive post-processing. While extrusion is efficient for uniform cross-sections, forging is preferable for parts requiring superior strength, durability, and structural integrity.

The last step was the post-processing, where there were evaluated the stiffness and stress distributions of the optimized element. The final details were fixed by using Altair Inspire to refine the geometry and the surface of the piece, resulting in a more presentable project.

## 9 RESULTS AND DISCUSSIONS

As said before, they were studied two different cases, one with 0.4 mass fraction (case 1) and the other with 0.2 (case 2). For this reason the results will be presented in parallel, thus to highlight and understand the differences between them. From a first analysis it was clear that the density distribution was not the opportune one in fact, as it is possible to see from the next table, there were an high percentage of elements with density between 10 % to 90 %.

Case 1 (0.4)		Case 2 (0.2)	
Normalised density $\rho$	Distribution in percentage (%)	Normalised density $\rho$	Distribution in percentage (%)
0.0 - 0.1	58.1	0.0 - 0.1	79.9
0.1 - 0.9	11.2	0.1 - 0.9	10.2
0.9 - 1.0	30.7	0.9 - 1.0	9.9

Figure 9.1. Percentage distribution of the continuous normalised density of the elements

For this reason, it was necessary to discretize the model, using a threshold set at 0.1, which drastically divide the elements as void (if the density is lower than this value) and as full for the other cases. This specific value of the threshold was chosen from the analysis of the Iso to guarantee the continuity and the quality of the mesh. A FEA was done on this configuration to verify if the structure was able to satisfy the requirements of the minimization. Below are reported for both toe and camber the FEM with displayed the magnitude of the rotations.

### 9.0.1 Case 1 (mass fraction 0.4)

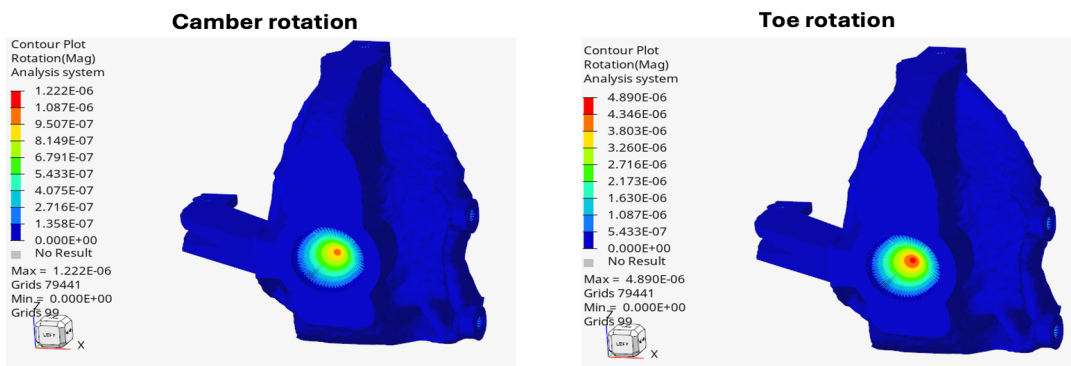


Figure 9.2. FEM with the magnitude of rotation for m.f. 0.4

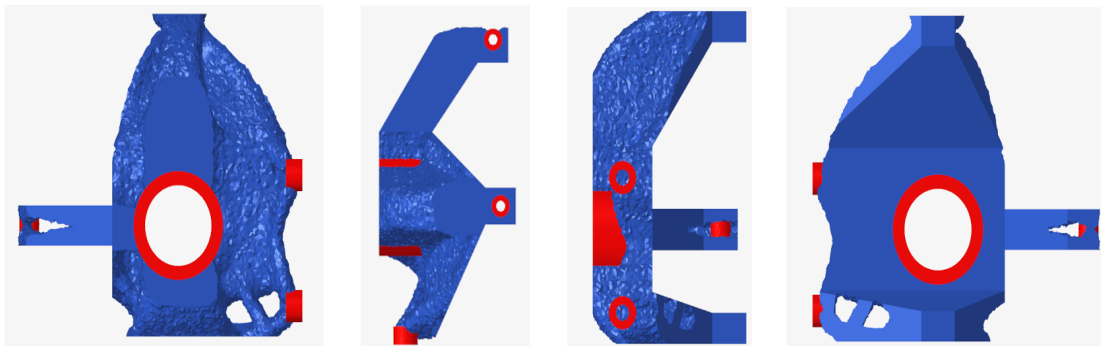


Figure 9.3. Optimized structure for m.f. 0.4

### 9.0.2 Case 2 (mass fraction 0.2)

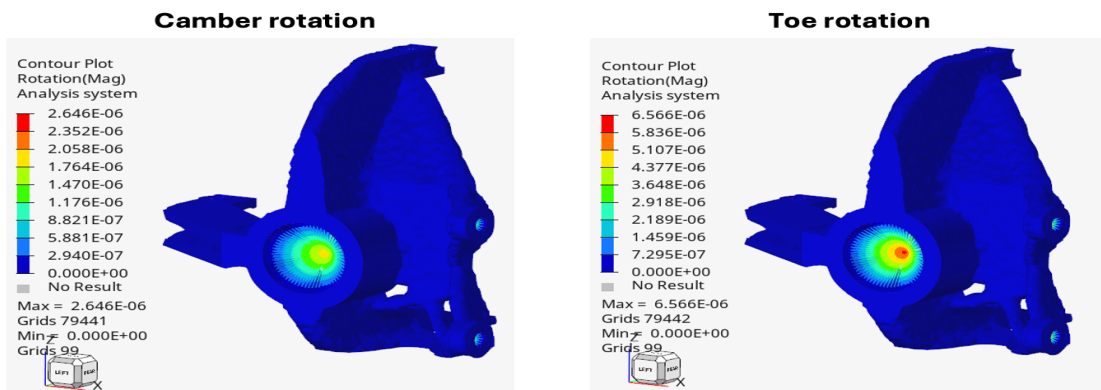


Figure 9.4. FEM with the magnitude of rotation for m.f. 0.2

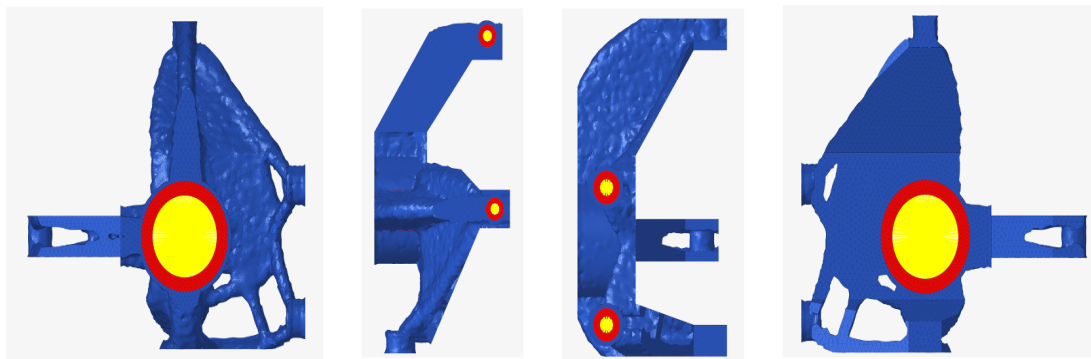


Figure 9.5. Optimized structure for m.f. 0.2

The following table presents the obtained results from the optimization:

Response	Case 1	Case 2	Objective/Constraint Value
Weighted compliance	79.25	203.56	Minimum
Mass Fraction	0.4	0.2	< [0.4, 0.2] (active cons.)
Toe Stiffness (Rot Z)	$4.890 \times 10^{-6}$ rad	$6.566 \times 10^{-6}$ rad	< $1.190 \times 10^{-5}$ rad
Camber Stiffness (Rot X)	$1.222 \times 10^{-6}$ rad	$2.646 \times 10^{-6}$ rad	< $6.250 \times 10^{-6}$ rad

Figure 9.6. Results for the 2 studied cases

The weighted compliances were obtained respectively in 24 and 45 iterations. This was probably due to the more relaxed constraint for the case 1, which ensures a faster convergence. As expected the most critical case is the one with lower mass fraction, in fact having less mass it is more difficult to make the structure stiffer. In particular between the two situations the stiffness increases of 2.6 times, the toe and camber angle decrease respectively of 26 % and 54 % with a double value of mass fraction. It is also clear that the toe and camber rotations are not active constraints because they do not reach the limit values for both the cases.

Another interesting point to notice is that the discretization procedure obviously compromised the final relation, in fact after this step the masses fraction (optimized mass / non-optimized mass) change from the defined ones accordingly to the table:

Component	Mass [kg]	Mass Fraction [-]
Original (solid domain)	2.089	1
Discretized solution	Case 1 (0.4 m.f.)	0.485
	Case 2 (0.2 m.f.)	0.282

Figure 9.7. Masses and masses fraction of the designs

In the end, with the optimization process the masses are reduced of 50 % for the first case, and of 70 % for the other case.

In order to obtain a more presentable piece, through wrapping and smoothing it was possible to end up with the following final refined design of the hub carrier.

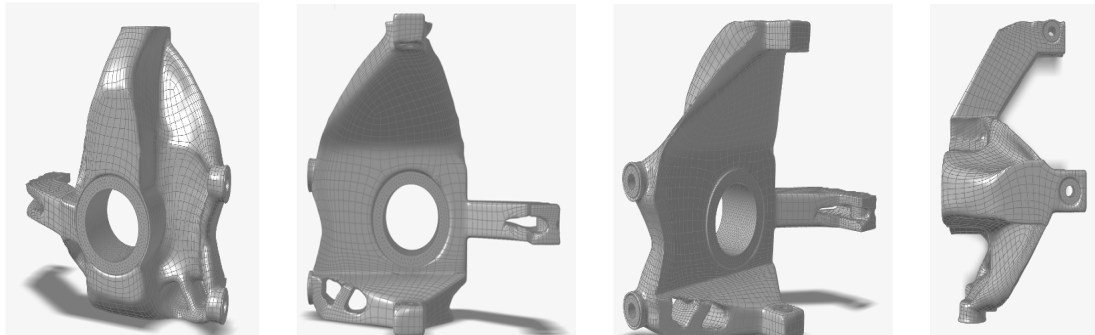


Figure 9.8. Refine structure for m.f. 0.4

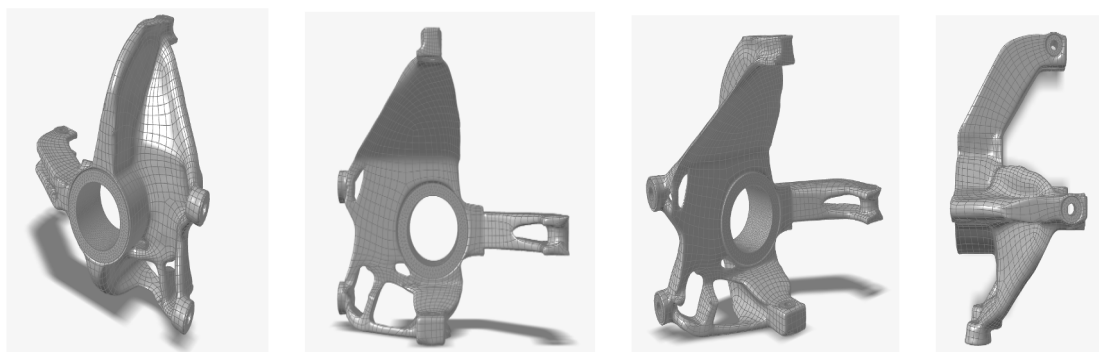


Figure 9.9. Refine structure for m.f. 0.2

## 10 FEA - STRESSES ANALYSIS

The loading conditions defined above, are tested in order to understand the magnitudes of von Mises equivalent stress all over the piece. The magnitudes are reported without the sign because the principal aim of this procedure is to highlight the highest stressed, identifying the the most critical zones.

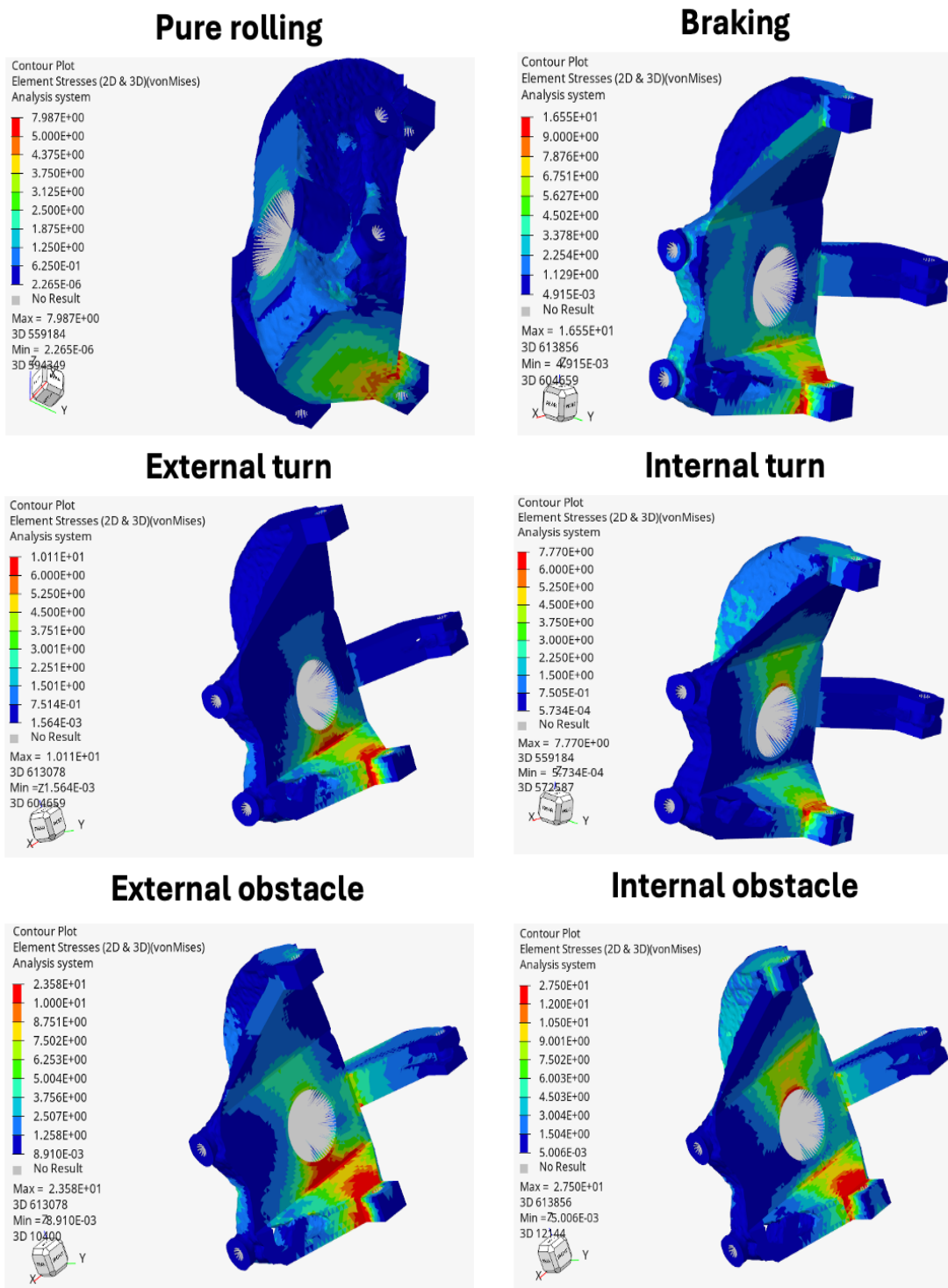


Figure 10.1. FEAs of the loading conditions for m.f. 0.4

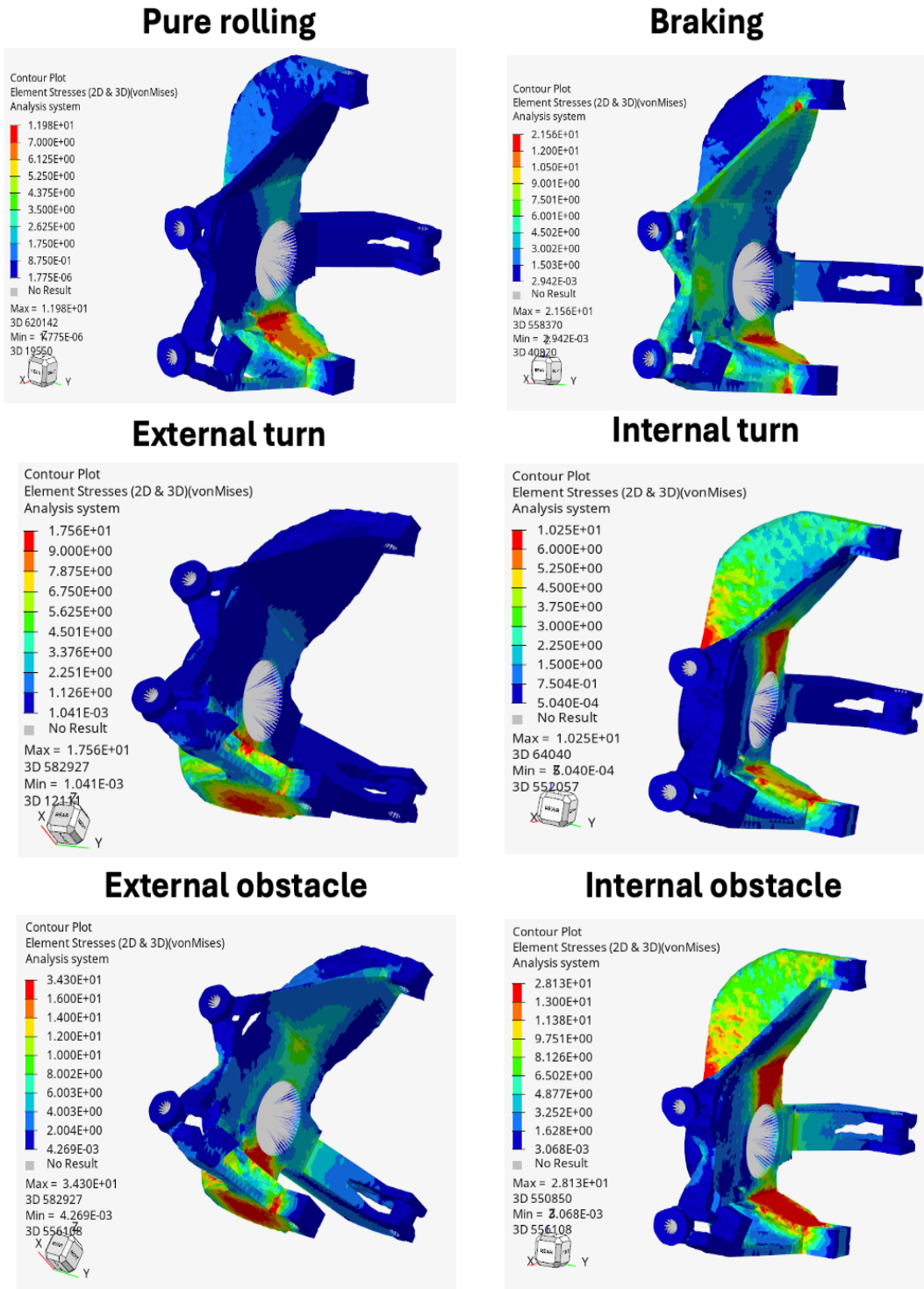


Figure 10.2. FEAs of the loading conditions for m.f. 0.2

Looking at the next table the situation is more clear:

Loading conditions	Von Mises stress [MPa]		Percentual increase
	Case 1 (0.4)	Case 2 (0.2)	
Pure rolling	7.98	11.98	33 %
Braking	16.55	21.56	23 %
External turn	10.11	17.56	42 %
Internal turn	7.77	10.25	24 %
External obstacle	23.58	34.30	31 %
Internal obstacle	27.50	28.13	2 %

Figure 10.3. Stresses variation for the loading conditions

As expected, the case with the highest stresses is the one with lower mass fraction, in fact in all the loading conditions there is a percentual magnitude increases from 0.4 mass fraction to 0.2. The most stressed case are for both the internal turn (with about 8 MPa for the case 1 and 10 MPa for the second), where there are effectively forces with less magnitude compared to the others. While the most stressed situation changes for the 2 mass fractions, being the internal obstacle for the case 1 (with 27.5 MPa) and the external obstacle for the case 2 (with 34.3 MPa). The highest percentual increases in stress magnitude is in the external turn condition, with 42 % more of stress. In all the cases, we are well below the proof strength of  $Y_s = 270$  MPa, thus entirely within the elastic range. From the stress diagrams, it can be also observed that the highest stress values are at the bottom of the element in correspondence with the full 3D pin, which constraints along X, Y and Z directions.

## 11 CONCLUSIONS

Software tools for topological optimization, based on finite element discretization, are invaluable for solving complex engineering problems that would be nearly impossible to handle manually. However, their effectiveness relies not only on their computational power but also on the user's understanding of the underlying models and limitations. Human intervention remains essential, particularly in post-processing, where manual refinement transforms raw optimization results into meaningful, manufacturable designs.

The final results shows how for both the mass fraction cases the requirements of stiffness and stress are respected ensuring stability of the element under all the loading conditions. the final choice is so the lighter one, 0.2 mass fraction with which a 70 % of the mass reduction is reached (0.589 kg). The finite element analysis permits to get how the optimization process reinforced the most stressed regions.

In order to improve the properties of the element, a future improvement could be a post-forging heat treatment to improve the hardness, the toughness, and wear resistance.